machines

Article

Test Study of Seepage Characteristics of Coal Rock under Various Thermal, Hydraulic, and Mechanical Conditions

Yanlin Zhao [1,*], Qiang Liu [1], Liming Tang [2], Jian Liao [1], Le Chang [3], Xiaguang Wang [1], Yang Li [1] and Sheng Ren [1]

[1] School of Resources Environment and Safety Engineering, Hunan University of Science and Technology, Xiangtan 411201, China
[2] State Key Laboratory of Geohazard Prevention and Geoenvironment Protection, Chengdu University of Technology, Chengdu 610059, China
[3] Suzhou Industrial Park Suxiang Cooperation Zone, Suzhou 215143, China
[*] Correspondence: yanlin_8@163.com

Abstract: The seepage characteristics of rocks under conditions of multi-field activity have always been important in the field of rock mechanics. This study used the MTS815 multi-functional electro-hydraulic servo rock testing machine to conduct seepage tests on long-flame coal specimens under different confining pressures, water pressures, and temperatures. This paper presents and discusses the seepage characteristics of coal specimens under the action of thermal hydraulic mechanical multi-field combinations. Considering parameters such as volumetric strain, temperature, thermal expansion coefficient, and initial porosity, the relationships of each parameter with porosity were obtained. The test results revealed that the volumetric strain of coal specimens increased gradually with the increase of temperature. The dynamic viscosity of water decreased with the increase of temperature, which accelerated the movement and circulation of water molecules. The increase in temperature caused the volume of the coal specimen to expand, the pores in the coal specimen squeezed against each other, the pore volume decreased, and the size of the seepage channel slowly decreased, which inhibited the seepage process. Furthermore, permeability gradually decreased with the increase of temperature. This inhibited the occurrence of seepage, and the higher the confining pressure, the lower was the permeability. The porosity of coal specimens decreased with the increase in temperature, which had an inhibitory effect on the seepage behavior. The results of this study provide experimental and theoretical support for the safe mining of coal and rock in underground mines.

Keywords: thermal-hydraulic-mechanical coupling; steady-state method; seepage; permeability; porosity

check for updates

Citation: Zhao, Y.; Liu, Q.; Tang, L.; Liao, J.; Chang, L.; Wang, X.; Li, Y.; Ren, S. Test Study of Seepage Characteristics of Coal Rock under Various Thermal, Hydraulic, and Mechanical Conditions. *Machines* **2022**, *10*, 1012. https://doi.org/10.3390/machines10111012

Academic Editor: Antonio J. Marques Cardoso

Received: 3 October 2022
Accepted: 28 October 2022
Published: 2 November 2022

1. Introduction

With the exhaustion of shallow coal deposits and other mineral resources, the search for resources continues deeper into the earth, and the extraction of deep resources has gradually become the new normal for resource development [1–3]. However, the geological conditions of deep resource mining are complex, involving increasing ground stress, rising ground temperature, rock mass fragmentation, karst water pressure intensifying water inrush, and frequent water disasters [4–6], potentially causing great safety hazards and affecting the progress of projects, resulting in the deterioration of the operational environment [7]. Problems such as increasing difficulty in resource extraction and the sharp increases in production costs [8] pose severe challenges for deep resource extraction. The mechanical and deformation properties of rock mass are different in the high temperature geothermal environment, and have a great impact on the mechanical properties of the rock during engineering, making water inrush accidents in mines more serious [9]. Therefore, it is of great practical significance for the safe operation of deep coal mining to carry out experimental research on the seepage of coal and rock mass under combined thermal hydraulic mechanical conditions.

The mining of deep mineral resources takes place in a geological environment characterized by complex effects of seepage, stress, and temperature [10]. The coal-mining process in this state of high geo-stress is affected by the seepage pressure and temperature of the groundwater in the surrounding rock mass. In this regard, scholars have carried out a series of studies on seepage, and performed seepage experiments under stress–seepage coupling. Bauer [11] discussed the effect of temperature on the physical and mechanical properties of different granites (westerly granite, carbonaceous granite). Trice [12] carried out a thermal seepage test on diorite, and analyzed the relationships between temperature, wave velocity, and permeability. Zhang [13] measured the permeability of high-temperature-treated marble, and reported that the permeability increased significantly between 327 °C and 427 °C, suggesting a temperature threshold in this range. Hart [14] developed a combined temperature–percolation–stress model in which an increase in temperature causes changes in properties such as elastic modulus, volume, compression coefficient, and cohesion between particles within the rock mass. Most notably, increase in temperature caused changes in the dynamic viscosity and density of water, resulting in changes in the percolation field. Zhao et al. [15,16] conducted an experimental study on the seepage characteristics of limestone under the action of hydraulic coupling and obtained the permeability characteristics of limestone under full stress–strain, as well as the damage and failure law of rock mass under hydraulic pressure. Zhang et al. [17,18] used steady state and transient methods to explore the law of seepage characteristics of red sandstone under different temperatures and stress environments. Wang et al. [19] conducted triaxial compression testing of coal under the action of thermal mechanical coupling, and studied the changes in deformation characteristics of coal and rock mass at high temperature, describing the volume expansion coefficient and elastic modulus. Feng et al. [20] carried out an experimental study on the deformation characteristics of anthracite coal under the action of thermal mechanical coupling and concluded that the thermal mechanical coupling action and pyrolysis gas production were the key factors affecting the deformation of coal mass. Wang [21] conducted compression tests on raw coal under thermal mechanical coupling, obtained thermal deformation parameters of coal specimens, and analyzed the thermal mechanical coupling effect on the thermal failure and instability mechanisms of deep coal and rock bodies. Li [22] used methane gas as the permeable medium and conducted seepage tests under different temperatures and stress conditions. Analysis revealed that stress had a compressive effect on the pores of the coal rock mass, and temperature influenced external expansion and internal expansion of the coal rock mass. Li et al. [23] used adsorbed methane gas and the non-adsorbed helium gas, respectively, to conduct coal seepage experiments under different stress conditions and different temperature conditions. The relationship between coal permeability and temperature under different effective stress conditions demonstrated neither linear increase nor decrease, and changes in the stress curve were apparent. Zhang et al. [24] used a servo-controlled high-temperature high-pressure triaxial rock-mass testing machine to study the permeability law of feldspar fine sandstone under constant pressure and temperature. The observed change was manifest in five characteristic stages. Yu et al. [25] conducted a seepage test on briquette samples, and studied the effects of confining pressure, axial pressure, and temperature on the permeability of briquette samples. It was found that temperature had a significant effect on the flow of gas in coal. Li et al. [26] described the relationship between porosity, permeability, and swelling deformation, considering the adsorption and deformation characteristics of coal seams. The greater the gas pressure in the coal seam, the greater the expansion deformation, the smaller the porosity, and the lower the permeability of the coal seam.

Based on the above research results, it can be stated that temperature, seepage force, and stress have obvious effects on changes in permeability and deformation during the process of coal and rock mass mining. However, many studies have only considered the isolated effect of different seepage water pressures, and have rarely comprehensively addressed temperature or the combined effect of seepage force and stress on the permeability characteristics of coal and rock mass. In addition, the commonly used seepage media are nitrogen and other gases. When the gas pressure difference is too small or the mass of the gas molecules is too light, the gas can no longer be regarded as a continuous fluid, and the mean free path of the gas molecules becomes greater than the pore size. The permeability obtained is smaller than the real situation. Based on this, this study used the MTS815 electro-hydraulic servo rock mechanics test system to carry out an experimental study on the influence of water and thermal mechanical coupling on changes in coal and rock permeability. We considered the evolution law of coal permeability with volumetric strain under different osmotic pressure, temperature, and confining pressure, and the expressions of volumetric strain, thermal expansion coefficient, and temperature are stated. The research results will provide an important reference for in-depth study, stability analysis, and safety evaluation of coal mining, considering the complex geological environment of high stress, high permeability, and hydraulic pressure in the surrounding rock.

2. Experimental Procedure

2.1. Specimen Preparation and Porosity Testing

The long-flame coal specimens were taken from the coal seam at a mining depth of 700 m in Houwenjialiang Coal Mine, Yijinhuoluo Banner, Ordos, China. According to the regulations [27], a cylindrical standard specimen was prepared with a size of 50 mm $\times$ 100 mm, the end of the specimen was ground to ensure that the parallelism and perpendicularity were controlled within $\pm$0.02 mm. The prepared specimen was flat at both ends, smooth on the side, and without drilling traces (see Figure 1). The coal rock specimens were then tested for porosity. An AiniMR-60 nuclear magnetic resonance test instrument was used to test the porosity of the specimens. The measurement results showed that the porosity of the coal rock specimens ranged from 14.70% to 15.72%, and the average porosity was 15.38%.

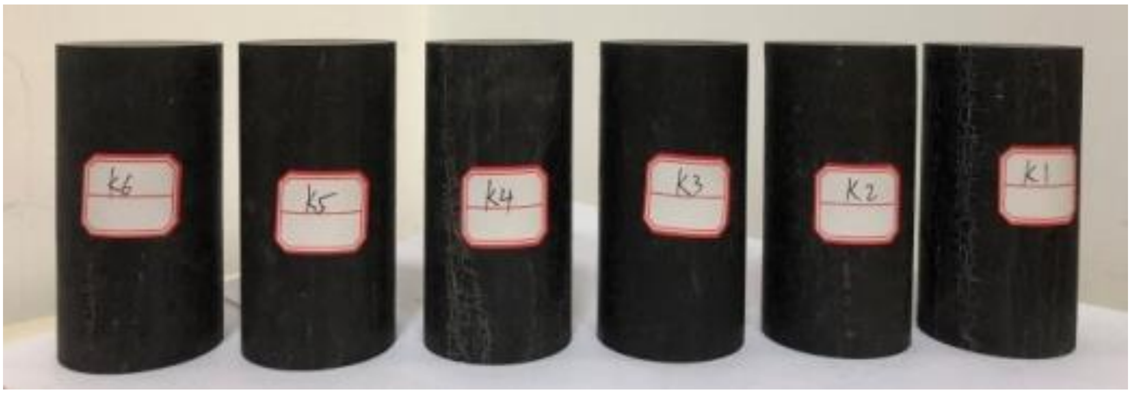

Figure 1. Standard coal specimens.

2.2. Testing Equipment and Principle

The seepage test was completed on the MTS815 electro-hydraulic servo rock mechanics test system in the Rock Mechanics Laboratory of Hunan University of Science and Technology (see Figure 2). This instrument can perform uniaxial compression tests, conventional triaxial compression tests, seepage tests, stress–seepage coupled tests, etc. The test system has four sets of independent closed-loop servo control systems, for axial pressure, confining pressure, pore water pressure, and temperature, respectively. The extensometer for measuring axial deformation and hoop deformation can work accurately and normally under high temperature and high pressure, to realize accurate measurement of fracture closure.

To obtain the variation law of the permeability characteristics of coal rocks under combined heat–water–force conditions, the steady-state method was employed in this experiment to determine the permeability of coal rocks. The computational principle of the steady-state method test was based on Darcy's law and made the following assumptions [28]: (1) The seepage medium is an incompressible fluid; (2) The distribution of primary cracks and pores in the rock mass is relatively uniform, and the rock mass can be regarded as a porous medium; (3) Constant seepage at stable pressure is regarded as continuous seepage; (4) The seepage in the stress–strain process conforms to Darcy's law. The expression to calculate the permeability of coal rock specimens can be stated as [29]:

$$K = \frac{\mu L \Delta Q}{A \Delta P \Delta t} \tag{1}$$

where K is the average permeability of coal rock in time Δt, m^2; ΔQ is the volume of water flowing through the coal rock specimen in the time, m^3; Δt is the time interval, s; μ is the viscosity coefficient of the fluid (water), Pa•s; A is the cross-sectional area of the coal rock specimen, m^2; L is the height of the rock specimen, m; ΔP is the osmotic pressure difference between the upper and lower ends of the coal specimen.

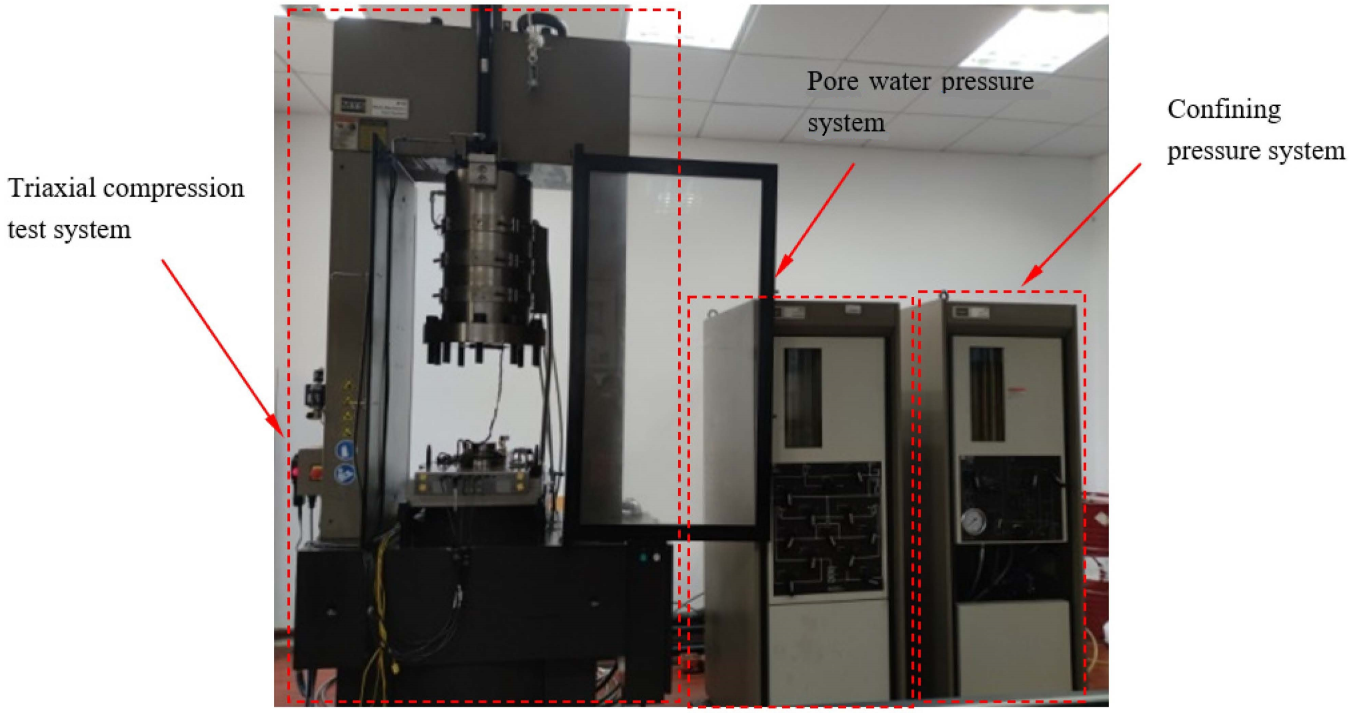

Figure 2. MTS815 rock multi-function electro-hydraulic servo testing machine.

2.3. Test Plan and Steps

For this test, the confining pressures were set to 5 MPa, 10 MPa, 15 MPa, and 20 MPa, for a total of four series. To form a pressure difference with the confining pressure and in order not to cause macroscopic damage to the coal rock, the specimen was placed in an environment with a triaxial stress difference of 5 MPa, and the axial pressure was applied in four series of 10 MPa, 15 MPa, 20 MPa, and 25 MPa, respectively. The water pressure was 4 MPa, 8 MPa, 12 MPa, and 16 MPa respectively; the temperature was set to 25 °C, 45 °C, 65 °C, and 85 °C, a total of four series. The seepage test on long-flame coal specimens was carried out under combined thermal hydraulic mechanical conditions. The main loading steps are as follows.

(1) The surrounding of the coal rock specimen was wrapped with a heat-shrinkable tube, the specimen was placed in the test system, the water pipe, axial extensometer, axial circumferential extensometer and temperature sensor were install, and the triaxial cell was positioned, as shown in Figure 3.
(2) A lower axial pressure of 3 kN was first preloaded in the axial direction, and then the confining pressure σ_3 and the axial pressure σ_1 were applied in turn at a loading rate of 2 MPa/min to obtain the experimental design value, and $\sigma_1 = \sigma_3$ was maintained. The hydraulic pressure was applied at a loading rate of 0.1 MPa/min to obtain the test design value P, ensuring that $\sigma_3 > P$, maintaining the axial pressure, confining

pressure, and water pressure. The water outlet time and water quality were recorded after the water flowed out of the lower outlet. The mass was weighed using a high-precision electronic balance, as shown in Figure 4. The electronic balance was connected to the computer to automatically record the data, and the program was run for 1.5 h after the water was stable.

(3) The temperature was increased from room temperature of 25 °C to 85 °C at a heating rate of 0.5 °C/min, and each level was loaded at 20 °C. Data including axial displacement, circumferential displacement, and temperature were monitored during the test.

Figure 3. Installation diagram of seepage test specimen.

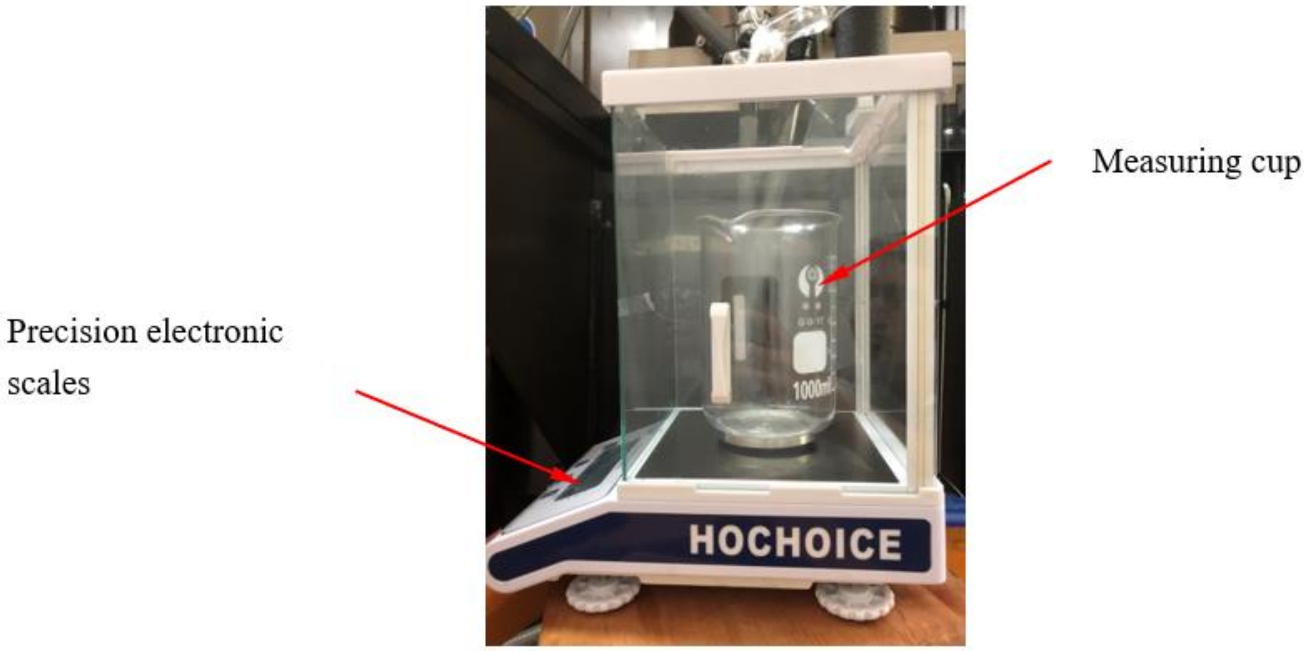

Figure 4. Outlet water collection device.

3. Test Results and Analysis

3.1. The Effect of Temperature on Volumetric Strain

The interior of coal rock mass is not a dense structure, and contains tiny cracks caused by pores and damage. Deep coal and rock bodies are often located in environments of high in situ stress and high temperature, where they are subject to the interaction of stress and temperature. The pores and fissures inside the coal rock mass undergo compression or expansion, affecting the volumetric strain, porosity, and permeability of the coal rock mass. Usually, the volumetric strain under triaxial stress conditions can be expressed as [30]:

$$\varepsilon_v = \varepsilon_1 + 2\varepsilon_3 \tag{2}$$

where ε_1 is the axial strain value; ε_3 is the radial strain value.

Figure 5 presents the volumetric strain–temperature–time curves of coal specimens at different temperatures. In the figure: ① water pressure point; ② normal temperature 25 °C stage; ③ 25–45 °C heating stage; ④ 45 °C constant temperature stage; ⑤ 45–65 °C heating stage; ⑥ 65 °C constant temperature stage; ⑦ 65–85 °C heating stage. As seen in Figure 5, the volumetric strain–temperature–time curves under the combination of the three variables of water pressure, stress, and temperature at a confining pressure of 5 MPa were basically similar to those for the confining pressures of 10 MPa, 15 MPa, and 20 MPa, and the volumetric strain of the coal specimens was influenced by the temperature. Due to limited space, here we take the confining pressure 5 MPa and the water pressure 4 MPa as an example; when the coal rock was under hydrostatic pressure, water pressure was applied, as in Figure 5a ①. Water pressure of 4 MPa having been applied to the upper end of the coal specimen, the water gradually penetrated into the interior of the coal specimen, causing the compressed and crowded pores and fissures in the specimen gradually to open slightly, promoting further development and expansion of fissures. The volume strain of the coal specimen gradually increased, and the curve showed a small increase. Subsequently, when the effect of water pressure reached its limit, the pores and cracks in the coal specimen did not continue to open, nor were new cracks generated, and the volume of the coal specimen did not increase further. As the test continued, the volume strain gradually decreased and the volumetric strain–temperature–time curve showed a gradual decrease, which was due to the continuous compression and closure of the pores and fissures inside the coal specimen under creeping action, which compressed the volume of the coal specimen, as shown in ② in Figure 5a.

The temperature was raised from room temperature of 25 °C to 45 °C, as shown in ③ in Figure 5a. The volumetric strain of the coal specimen increased rapidly and significantly during the temperature increase, the volumetric strain–time curve rose sharply, the volumetric strain increased from -0.3×10^{-3} to 2.06×10^{-3}, and the ratio of the beginning the volumetric strain upon heating increased by 586.7%. This shows that the increase in temperature caused the coal matrix to expand rapidly outward, the volumetric strain increased gradually, and the volume of the coal specimen increased with the increase in temperature. Moreover, the reason for the significant difference in the trend of volumetric strain under confining pressure of 20 MPa compared with other cases is that the coal rock was prone to shear fracture under the action of high confining pressure and was in a fully plastic state. Under the interaction of temperature and water pressure, the formation of cracks in the coal rock was promoted, and the coal rock showed a tensile shear effect so that the volumetric strain gradually increased. During the heating stage of 65–85 °C, the volumetric strain decreased under the confining pressure of 15 MPa, which was caused by the structure of the coal rock itself. In the compacted state, the other part of the specimen was in a state characterized by distributed pores. With the increase in temperature, the compaction of the coal rock gradually increased. At this time, the effect of confining pressure was greater than that of temperature damage.

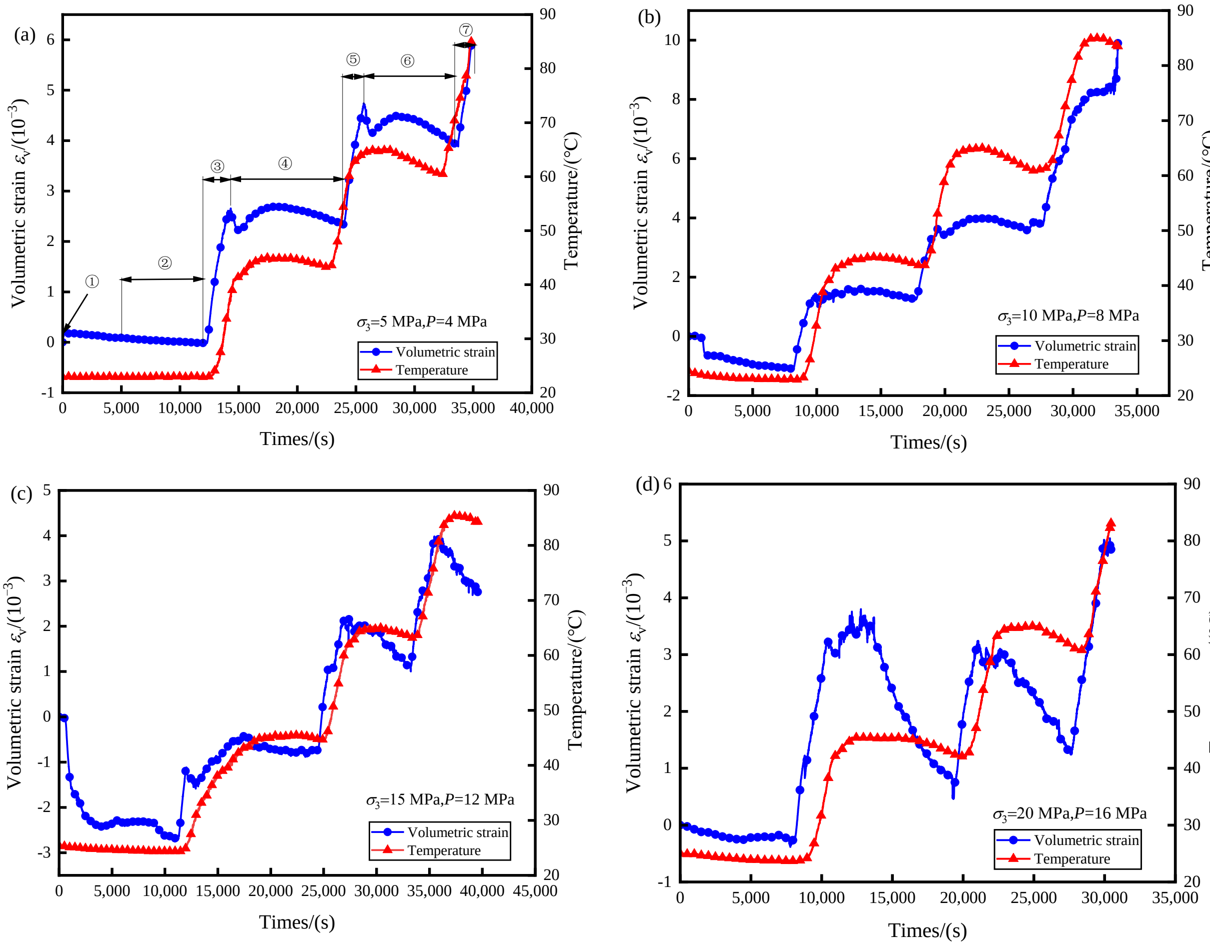

Figure 5. Volume–strain variation curve with temperature under different stress conditions with (**a**) σ_3 = 5 MPa, P = 4 MPa; (**b**) σ_3 = 10 MPa, P = 8 MPa; (**c**) σ_3 = 15 MPa, P = 12 MPa; (**d**) σ_3 = 20 MPa, P = 16 MPa.

In a constant temperature environment maintained at 45 °C, as shown in Figure 5a ④, the volumetric strain–time curve of the coal specimen exhibited a slight decrease. During the heating process, the cracks and pores inside the coal specimen opened rapidly. Under the restraint of confining pressure and axial pressure, some of the open cracks and pores were unable to expand outward indefinitely, so the cracks and pores in the open area were squeezed against each other, and the volume of the coal specimen decreased slightly.

As the temperature increased from 45 °C to 65 °C, as shown in ⑤ in Figure 5a, the volumetric strain of the coal specimens also increased significantly, from 2.46×10^{-3} to 4.16×10^{-3}, and the volumetric strain increased by 69.1%, which was less than the growth rate of volume strain from 25 °C to 45 °C.

The observations indicate that with the increase in temperature, the expansion effect of temperature on the internal cracks and pores of the coal specimen gradually weakened, and the increase of volume strain became smaller. While the temperature was maintained at 65 °C, as shown in Figure 5a ⑥, the volumetric strain of the coal specimen showed a similar change trend to when it was maintained at 45 °C. As the temperature continued to rise to 85 °C, as in Figure 5a ⑦, the volume strain of the coal specimen increased sharply by 45%. This was because the volume of the coal specimen expanded under the action of temperature, and the strength of the coal specimen was insufficient to resist the thermal expansion stress caused by the change of the temperature field. This resulted in the transformation of the coal rock mass from elastic deformation to plastic deformation, and the gradually increase of volumetric strain until the coal specimen was finally destabilized and damaged due to volume expansion.

Additionally, Figure 5 indicates that when the confining pressure was 5 MPa or 10 MPa, the volumetric strain of the coal specimen increased significantly, and the effect of volume expansion was more obvious; that is, the effect of thermal expansion stress generated by the temperature rise was more apparent. As the coal specimen was heated to 85 °C, the triaxial stress exerted on the coal specimen increased, it became more difficult for it to resist the stress generated by the temperature, the volumetric strain increased rapidly, and the coal specimen finally underwent large plastic deformation leading to instability and failure. When the confining pressure was 15 MPa or 20 MPa, although the volumetric strain of the coal specimen increased gradually as the temperature rose, the volume expansion was small due to the effect of triaxial stress. After the temperature reached 85 °C, although the volumetric strain of the coal specimen increased, the triaxial stress was sufficient to resist expansion caused by thermal stress. At a constant temperature of 85 °C, a section of the volumetric strain curve of the coal specimen indicated compression creep. This shows that under the multi-field thermal hydraulic mechanical combination, temperature played a leading role in changes of volumetric strain of coal specimens. In addition, the confining pressure inhibited the thermal expansion of the coal specimens under the action of temperature.

3.2. Influence of Temperature on Water Output in the Seepage Process

Using a high-precision electronic balance, the water quantities in the seepage process were measured at different temperature stages, and the flow velocity was obtained by differential calculation of water quantity. The flow-velocity–time–temperature curves were drawn for the coal specimens under different confining pressure and water pressure, as shown in Figure 6.

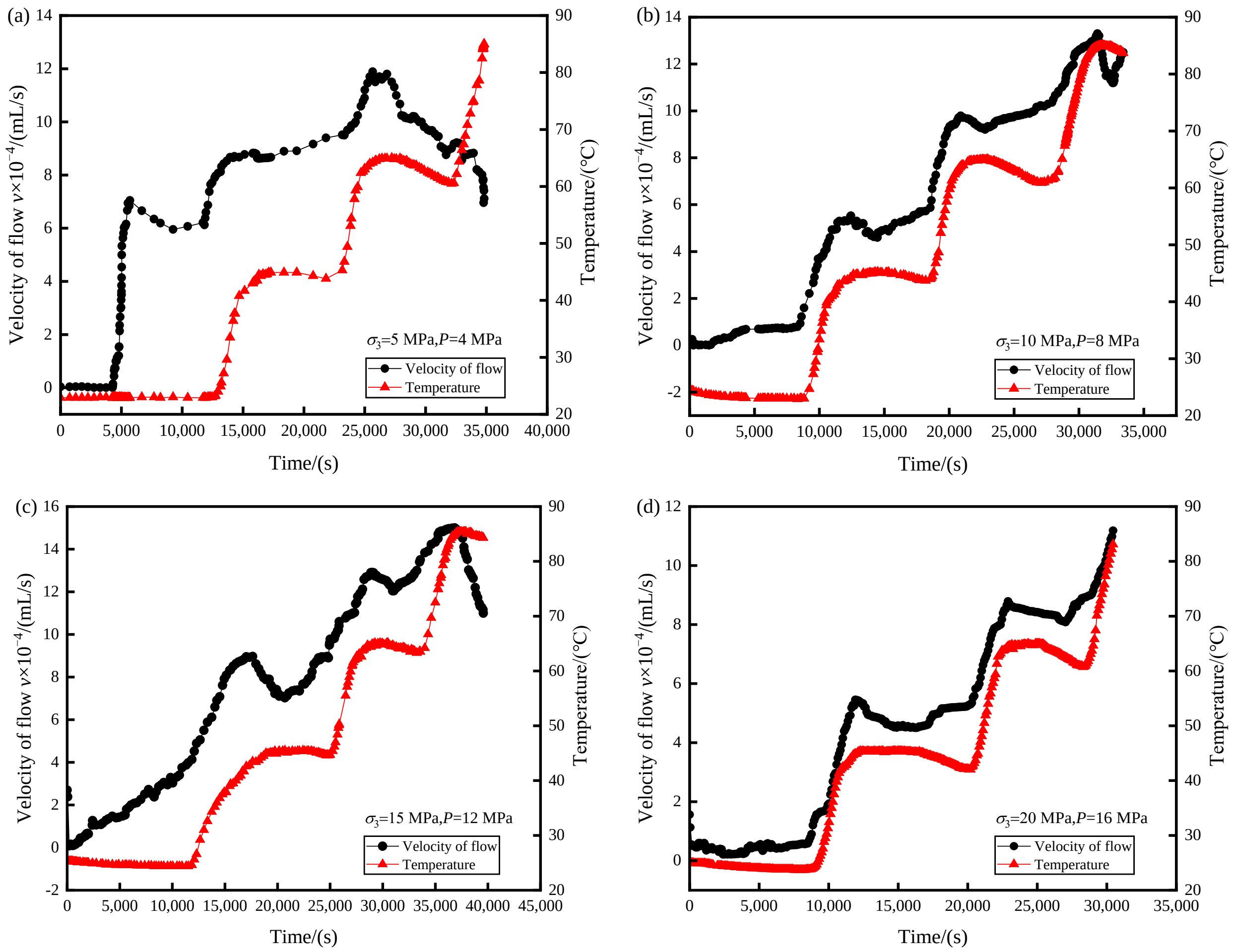

Figure 6. Variation law of temperature and flow rate with (**a**) σ_3 = 5 MPa, P = 4 MPa; (**b**) σ_3 = 10 MPa, P = 8 MPa; (**c**) σ_3 = 15 MPa, P = 12 MPa; (**d**) σ_3 = 20 MPa, P = 16 MPa.

As can be seen from Figure 6, when the confining pressure was 5 MPa, 10 MPa, 15 MPa or 20 MPa, the change trends of the velocity–time–temperature curves were roughly the same during the seepage test process. In each case, there was an increase followed by a small decrease in the velocity of water flow, due to the continuous action of the load. The volume compression of the coal specimen caused the internal cracks and pores to close, and the temperature increased under the lower confining pressure condition (σ_3 = 5 MPa), which significantly increased the water-production speed. This was mainly because the volume compression reduced the channels of water flow, and the dynamic viscosity of the water decreased, which accelerated the movement of water molecules and caused faster flow in the existing cracks and pores inside the coal specimen. As can be seen from the water velocity curve, the change was small in the early stage, showing an upward–downward trend. The main reason for this was that during the heating process, the interior of the coal specimen was not uniformly heated, resulting in different temperatures of water in the coal specimen, different dynamic viscosities of fluids at different positions in the coal specimen, and different rates of molecular diffusion. Additionally, the non-uniform temperature led to inconsistent thermal expansion around the coal specimen, and the fissures inside the coal specimen differed considerably, resulting in unstable velocity of outflowing water. When the internal temperature of the coal specimen was stable, the water entering the coal specimen was heated evenly, and the diffusion of water molecules was in a stable state so the water outlet velocity curve tended to rise steadily. Along with the increase in temperature, the effect of confining pressure was brought into full play, gradually decreasing the water flow speed. Under conditions of high confining pressure (σ_3 = 20 MPa), the water flow velocity curves at temperatures of 25 °C, 45 °C, and 65 °C were similar to the change results for confining pressure of 5 MPa, 10 MPa, and 15 MPa. As the temperature reached 85 °C, the water flow velocity curve of the coal specimen did not decrease but showed an upward trend. The main reason was that the coal specimen was in an environment of high triaxial stress, and the internal volume was relatively densely compressed. The creep interaction of coal specimens is complex, and the pore environment inside the coal specimen is changeable, which promotes the continuous increase of flow rate. The increase in water outlet velocity can be attributed to the increase in temperature, which reduced the dynamic viscosity of the water and accelerated the movement of water molecules, thus increasing the flow velocity inside the coal specimen. Therefore, the water outlet velocity gradually increased during the test.

3.3. The Effect of Temperature on the Permeability

As the temperature of the pore fluid changed, its viscosity coefficient also changed. Intermolecular dynamic viscosity is greatly affected by temperature, and changes in fluid viscosity have significant effects on the permeability of fluids [31]. According to the engineering toolbox, we calculated the dynamic water-viscosity value at each temperature stage. Figure 7 shows the change of the viscosity coefficient with temperature. When the temperature was 25 °C, the dynamic viscosity of the water was 0.89 mPa·s, and its dynamic viscosity at 85 °C was 0.3345 mPa·s. Thus, when the temperature was increased from 25 °C to 85 °C, the dynamic water viscosity decreased by about 1.66 times.

In order to ascertain the permeability of coal rock samples, the collected water output and the viscosity coefficient value in Table 1 were substituted into Equation (1), and the value of permeability *K* of coal rock was obtained. Figure 8 shows the change curve of the permeability of coal rock under different confining pressures. The results for coal sample permeability changes at different temperatures are shown in Table 2.

It can be concluded from Figure 8 that the permeability of coal specimens was greatly affected by temperature, and the permeability of coal specimens gradually decreased with the increase of temperature and confining pressure. When the confining pressure was 5 MPa and the temperature increased from 25 °C to 45 °C, the permeability of coal specimens decreased from 15.08×10^{-18} m^2 to 6.49×10^{-18} m^2; a decrease of about 56.9%. When the temperature of the coal specimen reached 65 °C, its permeability was about

3.64×10^{-18} m^2, about 43.9% lower than its permeability at 45 °C, a lower decrease than was observed in the previous heating stage. When the temperature reached 85 °C, the permeability of the coal specimen decreased to 2.94×10^{-18} m^2, which was 19.2% lower than the permeability at 65 °C, and 80.5% lower than at 25 °C. The main reason was that seepage occurred mainly in the fissures and pores of the coal rock mass. With the increase in temperature, although the volume of the coal specimen showed a trend of expansion, the internal expansion of the coal specimen was limited by the constraints of confining pressure and axial pressure. The generated cracks and pores squeezed against each other so they closed during the expansion process, the seepage channels were reduced, and the permeability showed a downward trend. When the confining pressure was 10 MPa, the permeability values at 25 °C, 45 °C, 65 °C, and 85 °C were 1.89×10^{-18} m^2, 1.48×10^{-18} m^2, 1.32×10^{-18} m^2, and 1.18×10^{-18} m^2, representing reduction rates of 21.7%, 10.8%, 10.6%, respectively. When the confining pressure was 15 MPa, the permeability values at 25 °C, 45 °C, 65 °C, and 85 °C were 1.59×10^{-18} m^2, 1.19×10^{-18} m^2, 1.02×10^{-18} m^2, and 0.91×10^{-18} m^2, respectively. The reduction rates were 25.1%, 14.2%, and 10.7%, respectively. When the confining pressure was 20 MPa, the permeability values at 25 °C, 45 °C, 65 °C, and 85 °C were 0.12×10^{-18} m^2, 0.18×10^{-18} m^2, 0.20×10^{-18} m^2, and 0.22×10^{-18} m^2, respectively. The magnitudes were −50%, −11.1%, and −10%, respectively. When the confining pressure reached as high as 20 MPa, the permeability properties of the coal specimens measured at the four recorded temperature stages were remarkably different from those obtained from other three sets of tests.

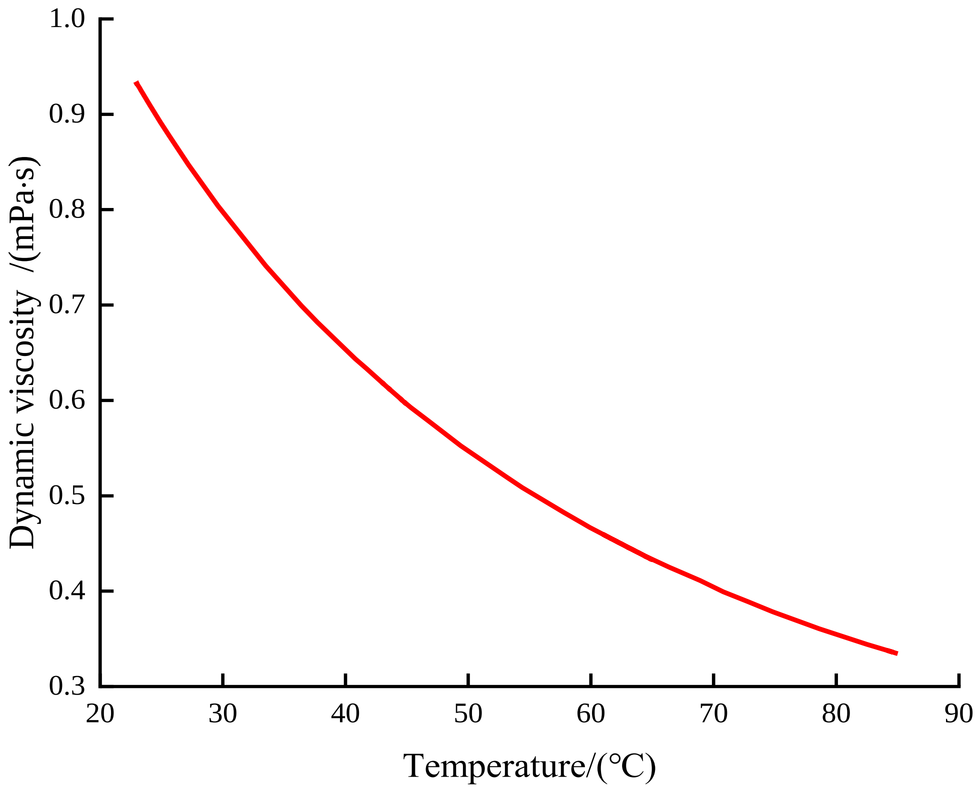

Figure 7. Variation curve of dynamic viscosity at different temperatures.

Table 1. Dynamic viscosity at different temperatures.

Temperature /°C	**25**	**45**	**65**	**85**
Dynamic Viscosity/mPa·s	0.8900	0.5958	0.4329	0.3345

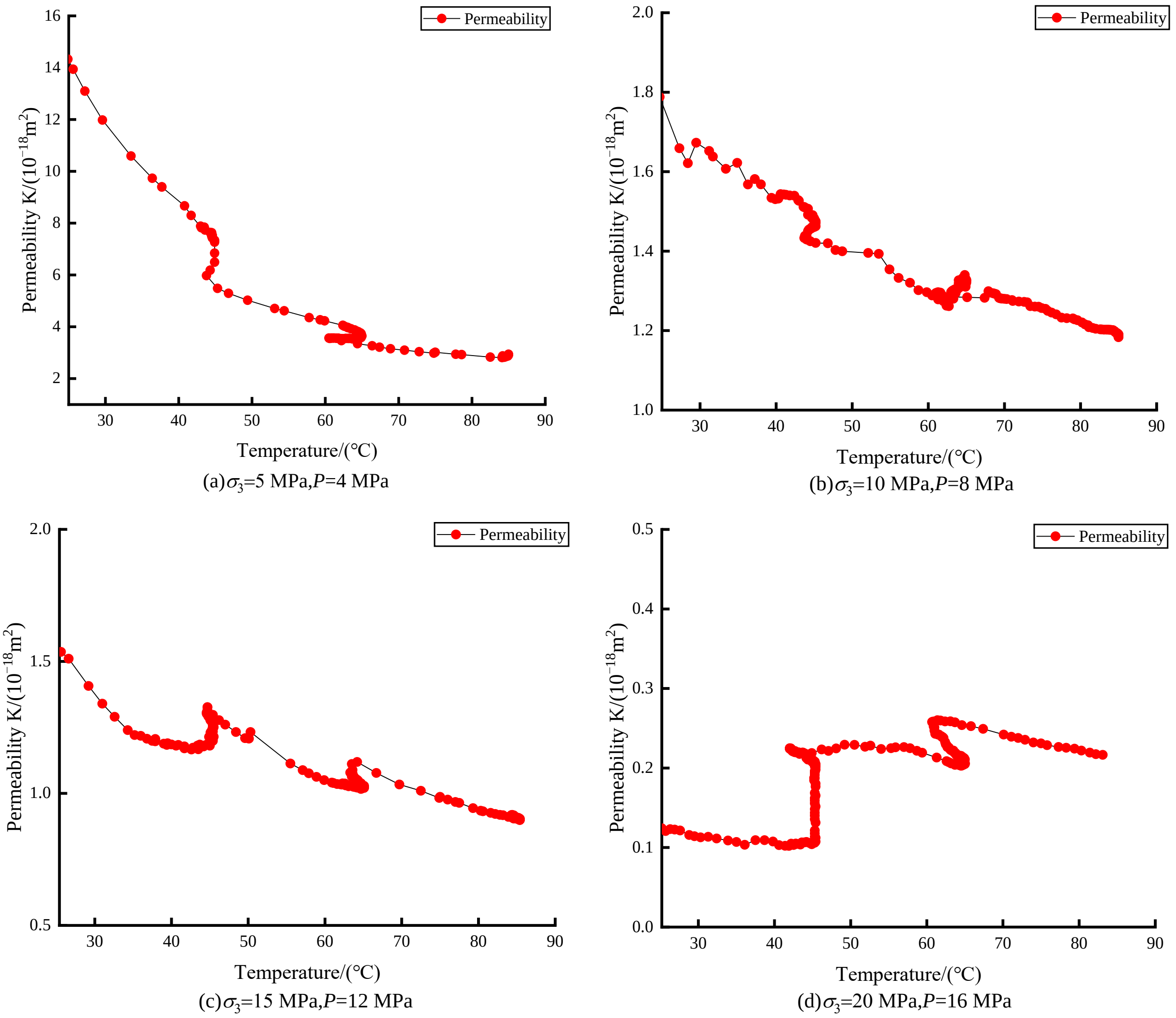

Figure 8. Curves of permeability change under different confining pressures.

Table 2. Permeability increase of coal specimens at different temperatures.

Confining Pressure/MPa	Hydraulic Pressure/MPa	Temperature /°C	Permeability /10^{-18} m^2	Rate /%
5	4	25	15.08	-
		45	6.49	−56.9
		65	3.64	−43.9
		85	2.94	−19.2
10	8	25	1.89	-
		45	1.48	−21.7
		65	1.32	−10.8
		85	1.18	−10.6
15	12	25	1.59	-
		45	1.19	−25.1
		65	1.02	−14.2
		85	0.91	−10.7
20	16	25	0.12	-
		45	0.18	50.0
		65	0.20	11.1
		85	0.22	10.0

When the temperature was raised from room temperature of 25 °C to 45 °C, the permeability increased from 0.12 × 10^{-18} m^2 to 0.18 × 10^{-18} m^2, a 1.5-fold increase, and when the temperature continued to rise to 65 °C, the permeability increased from 0.8 × 10^{-18} m^2 to 0.20 × 10^{-18} m^2, an increase of about 1.1 times. As the temperature increased to 85 °C, the permeability continued to increase to 0.22 × 10^{-18} m^2, which was about 10% higher than the permeability at 65 °C. This indicates that under high confining pressure, the coal specimen was compressed relatively densely, and the increase of water pressure was insufficient to increase the expansion of volume strain. With the increase in temperature, the volume expansion of coal specimens under high confining pressure was not obvious, and there were some seepage channels that had not closed.

However, the creep effect under temperature and stress complicated the internal environment of coal specimens, causing the changes in pore volume to become unstable, and the penetration rate showed an upward trend. This shows that the increase of temperature and the increase of confining pressure had an inhibitory effect on the permeability of the specimens. In addition, the permeability of the coal specimens at the same temperature continued gradually to decrease, and it can be considered that the increase of water pressure had no obvious effect on the permeability of coal specimens.

3.4. Evolution Analysis of Coal Porosity

During seepage testing, the coal specimen's porosity volume is related to its permeability. It was necessary to analyze further the porosity evolution law under combined thermal hydraulic mechanical action. The effective stress and water pressure of the coal specimen remained unchanged during the seepage process, and the porosity changed with the increase of temperature. The increase of temperature caused expansion and contraction in the volume of the coal specimen. The relationship between the porosity and the volume strain of the coal specimen can be expressed [32]:

$$\varphi_t = \frac{V_{p0} + \Delta V_p}{V_{t0} + \Delta V_t} = \frac{V_{t0} + \Delta V_t - V_{g0} - \Delta V_g}{V_{t0} + \Delta V_t} = 1 - \frac{1 - \varphi_0}{1 - \varepsilon_V}\left(1 + \frac{\Delta V_g}{V_{g0}}\right) \tag{3}$$

In the formula, φ_t is the porosity of the coal specimen; V_{p0} is the original pore volume of the coal specimen; ΔV_p is the increment of the pore volume; V_{t0} is the original volume of the coal specimen; ΔV_t is the volume increase of the coal specimen; V_{g0} is the original volume of the coal matrix; ΔV_g is the volume change of the coal matrix; φ_0 represents the initial porosity of the coal specimen; ε_v is the volumetric strain of the coal specimen.

Figure 9 shows the volume expansion diagram of coal matrix particles; σ_a is the external triaxial stress and σ_b is the internal thermal expansion stress.

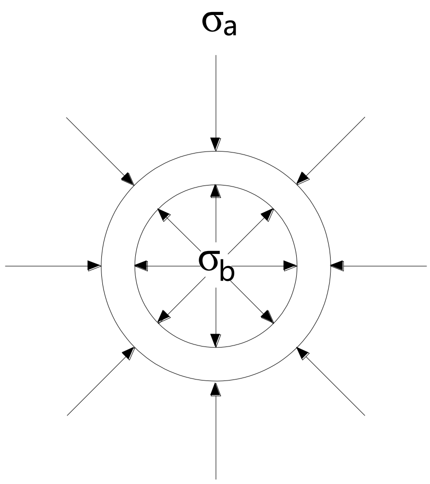

Figure 9. Thermal expansion diagram of coal matrix particle volume.

The volume expansion of coal particles is quantified as:

$$\frac{\Delta V_g}{V_{g0}} = \beta_g \Delta T \tag{4}$$

where β_g is the coefficient of thermal expansion of the coal specimen in the elastic phase; ΔT is the change in temperature.

Substitute Equation (4) into Equation (3) to obtain the porosity after the interaction between the temperature change, the volume strain of the coal specimen, and the thermal expansion coefficient in the elastic stage:

$$\varphi_t = 1 - \frac{1-\varphi_0}{1-\varepsilon_V}(1+\beta_g \Delta T) \tag{5}$$

Under the effect of thermal mechanical coupling, the axial thermal expansion coefficient of long-flame coal increases gradually with the increase of temperature without exceeding the temperature threshold, and the thermal expansion coefficient can be expressed as:

$$\beta_g = \frac{\Delta V}{\Delta T V_0} = \frac{V_1 - V_0}{\Delta T V_0} \approx \frac{\varepsilon_V}{\Delta T} \tag{6}$$

Substituting Equation (6) into Equation (5), the relationship between porosity and volumetric strain can be stated as:

$$\varphi_t = 1 - \frac{1-\varphi_0}{1-\varepsilon_V}(1+\varepsilon_V) \tag{7}$$

It can be seen from Equation (7) that the porosity of the coal specimen is related only to the volumetric strain. The volumetric strain of the coal specimens changed gradually during the temperature increase, which in turn caused the porosity to change. Substituting the volumetric strain values at different temperatures into Equation (7), the values of coal specimen porosity at each temperature were obtained, and a graph of porosity variation with temperature is shown in Figure 10.

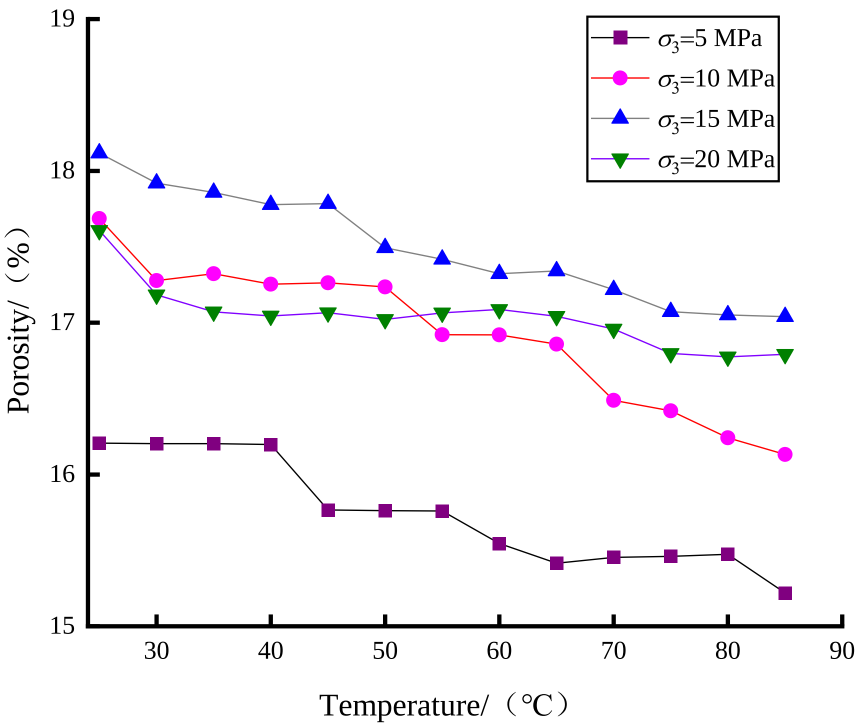

Figure 10. Calculated values of porosity at different temperatures.

It can be seen from Figure 10 that with the increase of temperature, the porosity values of coal specimens at 25 °C, 45 °C, 65 °C, and 85 °C gradually decreased, and the porosity was negatively correlated with temperature. Taking the confining pressure of 20 MPa as an example, the changes of coal specimens' porosity were small, and the porosity of coal specimens hardly changed at 45 °C or 65 °C, while the permeability values were quite different at these two temperature values. When the temperature reached 85 °C, the porosity of the coal specimen decreased greatly, which was reflected in changes in the permeability. Although the porosity of the coal specimen decreased, the volume of the coal specimen was compact and the pore volume decreased, while the increase in temperature caused the coal specimen to expand slightly, which helped to form seepage channels. The results show that under high confining pressure the permeability increased slightly with increase temperature. The porosity under confining pressure of 20 MPa was higher than under 5 MPa, because under conditions of axial force and high confining pressure, coal rock is more prone to cracking, and the cracks squeeze against each other to form tiny voids. As a result, the porosity gradually decreased. With the increase in temperature, the coal rock was subjected to thermal damage, and the porosity increased while the internal structure of the coal was partially dense and partially cracked. However, under confining pressure of 5 MPa, there were fewer cracks in the coal rock, the cracks were squeezed against each other to form narrow spaces, and the porosity gradually decreased.

Generally, the seepage testing under combined thermal hydraulic mechanical conditions showed that the permeability of coal specimens decreased gradually with the increase of temperature. The main reason was that the increase of temperature made the volume of the coal specimen expand. When the expansion reached a certain value limit, the cracks and pores in the coal specimen were squeezed and closed, and the porosity gradually decreased, which hindered the seepage medium during the seepage process, and the permeability decreased. The results demonstrate that the temperature increase during the seepage testing inhibited the seepage behavior of coal specimens to a certain extent.

4. Conclusions

(1) With the increase of temperature, the volumetric strain of the coal specimens increased gradually, and the expansion of volume was obvious. The higher the temperature, the greater was the increase of volumetric strain. The increase of the confining pressure had an inhibitory effect on the thermal expansion of the coal specimens. The thermal expansion of coal specimens under the action of high confining pressure was not obvious, and the volume strain increased slightly.

(2) Temperature had an inhibitory effect on the seepage of coal specimens. The higher the temperature, the lower was the permeability. The increase in temperature caused the coal matrix to heat and expand, and the internal cracks and pores of the coal body were compressed and closed. The higher the temperature, the more pores and fractures were closed, and fewer seepage channels remained present, therefore the permeability was reduced. Confining pressure also had an inhibitory effect on seepage. Under the same temperature conditions, the greater the confining pressure, the lower was the permeability. The increase of the confining pressure caused the coal specimen volume to compress and become compact, so increasing the water pressure did not significantly increase the permeability of coal specimens.

(3) Considering parameters such as volume strain, temperature, thermal expansion coefficient, and initial porosity, the relational expressions for porosity under each parameter were deduced. Moreover, the results of the seepage test were compared with the theoretically calculated values, and it was found that the theoretically calculated values were consistent with the experimental values. Except for when the confining pressure was 20 MPa, the porosity and permeability of coal specimens decreased with the increase in temperature.

Author Contributions: Methodology, Y.Z.; Investigation, J.L., L.C. and X.W.; Formal analysis, L.T., Y.L. and S.R.; Writing—original draft, Q.L.; Funding acquisition, Y.Z.; Writing—review and editing, Y.Z. All authors have read and agreed to the published version of the manuscript.

Funding: This research was funded by the National Natural Science Foundation of China (Nos. 52274118, 51774131), and Graduate Research and Innovation Projects of Hunan Province (No.CX20221042). The authors are thankful for all of the support for this basic research.

Data Availability Statement: The data that support the findings of this study are available from the corresponding author upon reasonable request.

Conflicts of Interest: The authors declare no conflict of interest.

References

1. Xie, H.P. Research review of the state key research development program of China: Deep rock mechanics and mining theory. *J. China Coal Soc.* **2019**, *44*, 1283–1305.
2. Wu, Q.H.; Weng, L.; Zhao, Y.L.; Feng, F. Influence of infilling stiffness on mechanical and fracturing responses of hollow cylindrical sandstone under uniaxial compression tests. *J. Cent. South Univ.* **2021**, *28*, 2485–2498. [CrossRef]
3. Wang, M.; Wan, W.; Zhao, Y.L. Experimental study on crack propagation and coalescence of rock-like materials with two pre-existing fissures under biaxial compression. *Bull. Eng. Geol. Environ.* **2020**, *79*, 3121–3144. [CrossRef]
4. Xue, D.J.; Zhou, H.H.; Wang, C.S.; Li, D.P. Coupling mechanism between mining-induced deformation and permeability of coal. *Int. J. Min. Sci. Technol.* **2013**, *23*, 783–787. [CrossRef]
5. Ohnishi, Y.; Kobayashi, A. Thermal–hydraulic–mechanical coupling analysis of rock mass. In *Analysis and Design Methods*; Pergamon: King of Prussia, PA, USA, 1993; pp. 191–208.
6. Liu, J.H.; Zhao, Y.L.; Tan, T.; Zhang, L.Y.; Zhu, S.T.; Xu, F.Y. Evolution and modeling of mine water inflow and hazards characteristics in southern coalfields of China: A case of Meitanba mine. *Int. J. Min. Sci. Techno* **2022**, *32*, 513–524. [CrossRef]
7. Li, P.; Rao, Q.H.; Li, Z.; Jing, J. Thermal-hydro-mechanical coupling stress intensity factor of brittle rock. *Trans. Nonferr. Met. Soc. China* **2014**, *24*, 499–508. [CrossRef]
8. Kong, H.L.; Miao, X.X.; Wang, L.Z.; Zhang, Y.; Chen, Z. Analysis of the Harmfulness of Water-Inrush from Coal Seam Floor Based on Seepage Instability Theory. *J. China Univ. Min. Technol.* **2007**, *17*, 453–458. [CrossRef]
9. Brace, W.F.; Walsh, J.B.; Frangos, W.T. Permeability of granite under high pressure. *J. Geophys. Res.* **1968**, *73*, 2225–2236. [CrossRef]
10. Louis, C. Rock Hydraulics. In *Rock Mechanics*; Springer: Vienna, Austria, 1972.
11. Bauer, S.J.; Johnson, B. Effects of slow uniform heating on the physical properties of the westerly and charcoal granites. In Proceedings of the U.S. Symposium on Rock Mechanics, Austin, TX, USA, 4–6 June 1979.
12. Trice, R.; Warren, N. Study of the correlation of acoustic velocity and permeability of granodiorites from the Valles Caldera, New Mexico. *EOS Trans. Am. Geophys. Union* **1976**, *57*, 12.
13. Zhang, S.; Paterson, M.S.; Cox, S.F. Microcrack growth and healing in deformed calcite aggregates. *Tectonophysics* **2001**, *335*, 17–36. [CrossRef]
14. Hart, R.D.; St John, C.M. Formulation of a fully-coupled thermal-mechanical-fluid flow model for non-linear geologic systems. *Int. J. Rock Mech. Min. Sci. Geomech.* **1986**, *23*, 213–224. [CrossRef]
15. Zhao, Y.L.; Liu, Q.; Liu, H. Triaxial compression and acoustic emission tests on single cracked limestone and compression-shear fracture model under hydraulic-mechanical coupling action. *J. China Coal Soc.* **2021**, *46*, 3855–3868.
16. Zhao, Y.L.; Tang, J.Z.; Chen, Y.; Zhang, L.Y.; Wang, W.J.; Wan, W.; Liao, J. Hydromechanical coupling tests for mechanical and permeability characteristics of fractured limestone in complete stress-strain process. *Environ. Earth Sci.* **2017**, *76*, 1–18. [CrossRef]
17. Zhang, P.S.; Zhao, C.Y.; Hou, J.Q.; Li, T.H.; Zhang, X. Experimental study on seepage characteristics of deep sandstone under temperature-stress-seepage coupling conditions. *Chin. J. Rock Mechan. Eng.* **2020**, *39*, 1957–1974.
18. Zhang, P.S.; Zhao, C.Y.; Hou, J.Q.; Li, T.H. Experimental study on seepage characteristics of deep sandstone under high temperature and different hydraulic pressures. *Chin. J. Rock Mechan. Eng.* **2020**, *39*, 1117–1128.
19. Wang, X.; Feng, Z.J. Thermal deformation of long flame coal under thermos-mechanical coupling. *Coal Eng.* **2021**, *53*, 135–139.
20. Feng, Z.J.; Wan, Z.J.; Zhao, Y.S.; Li, G.W.; Zhang, Y.; Wang, C. Experimental investigation into deformation characteristics of anthracite under thermo-mechanical coupling conditions. *Chin. J. Rock Mechan. Eng.* **2010**, *29*, 1624–1630.
21. Wang, C.G.; Chen, L.J.; Wang, C.S.; Chen, L.-J.; Wang, C.-S.; Zhang, X.-H.; Wei, M.-Y. Experiment on thermal-induced expansion and mechanical properties of gas-bearing intact coal subjected to thermal-mechanical loading. *Soil Mechan.* **2014**, *35*, 1015–1024.
22. Li, Z.Q.; Xian, X.F. Study on experiment of coal permeability with temperature and stress changing. *J. Liaoning Tech. Univ. (Nat. Sci.)* **2009**, *28* (Suppl. S1), 156–159.
23. Li, Q.Z.; Xian, X.F.; Long, Q.M. Experiment study of coal permeability under different temperature and stress. *J. China Univ. Min. Technol.* **2009**, *38*, 523–527.
24. Zhang, Y.; Wan, Z.J.; Kang, J.R.; Zhao, Y.-S. Analysis of stage characteristics of sandstone permeability under conditions of temperature and triaxial stress. *Rock Soil Mech.* **2011**, *32*, 677–683.

25. Yu, Y.J.; Zhang, H.; Zhang, C.H.; Hao, Z.; Wang, L.-G. Effects of temperature and stress on permeability of standard coal briquette specimen. *J. China Coal Soc.* **2013**, *38*, 936–941.
26. Li, X.C.; Guo, Y.Y.; Wu, S.Y. Analysis of The Relation of Porosity, Permeability and Swelling Deformation of Coal. *J. Taiyuan Univ. Technol.* **2005**, *03*, 264–266.
27. The National Standards Compilation Group of the Peoples Republic of China. *GB/T 50266—99 Standard for Tests Method of Engineering Rock Masses*; China Planning Press: Beijing, China, 1999. (In Chinese)
28. Wang, W.; Xu, W.Y.; Wang, R.B.; Cao, Y.; Wang, H.; Feng, S. Permeability of dense rock under triaxial compression. *Chin. J. Rock Mech. Eng.* **2015**, *34*, 40–47. (In Chinese)
29. Goodman, R.E. *Introduction to Rock Mechanics*, 2nd ed.; Wiley: New York, NY, USA, 1989.
30. Chen, M.X. *Elasticity and Plasticity*; Science Press: Beijing, China, 2007.
31. Kestin, J.; Sokolov, M.; Wakeham, W.A. Viscosity of liquid water in the range $-8\,^{\circ}C$ to $150\,^{\circ}C$. *J. Phys. Chem. Ref. Data* **1978**, *7*, 941–948. [CrossRef]
32. Cheng, Y.P.; Liu, Q.Q.; Ren, T.X. *Coal Mechanics*; Science Press: Beijing, China, 2017.